

# A New Pyrazoline-Based Fluorescent Probe for Cu<sup>2+</sup> in Live Cells

Meng-Meng Li · Shu-Ya Huang · Hui Ye · Fei Ge ·  
Jun-Ying Miao · Bao-Xiang Zhao

Received: 14 December 2012 / Accepted: 24 February 2013 / Published online: 21 March 2013  
© Springer Science+Business Media New York 2013

**Abstract** A new pyrazoline-based probe was synthesized and the structure was determined by using X-ray diffraction analysis. The probe responds to Cu<sup>2+</sup> in aqueous medium in “turn-off” fluorescent manner with selectivity and sensitivity. Furthermore, the probe could be used for real-time tracking of Cu<sup>2+</sup> in Hela cells.

**Keywords** Pyrazoline · Fluorescent probe · Copper ion · Living cell · Imaging

## Introduction

Copper is an essential trace element in the human body and plays a pivotal role in a variety of many fundamental physiological processes in organisms [1–3]. However, Cu<sup>2+</sup> is high toxic to biological systems when Cu<sup>2+</sup> is at the high concentration exceeding cellular needs. It leads to severe

neurodegenerative diseases such as Menkes disease, Wilson disease, and Alzheimer’s disease [4–6]. Therefore, the highly selective, sensitive and rapid recognition of Cu<sup>2+</sup> in living cells is demanded.

Based on the different sensing methods for detecting Cu<sup>2+</sup>, fluorescent probes have several advantages over other methods due to their high sensitivity, selectivity and real-time monitoring [7–12]. In recent years, a number of studies on the design and synthesis of fluorescent probes for the detection of Cu<sup>2+</sup> ions have been reported and a lot of probes have been used with some success in biological applications [13–16]. Several “turn-off” fluorescent probes for Cu<sup>2+</sup> have also been reported to monitor Cu<sup>2+</sup> in biological applications [17, 18], but some of them have shortcomings for practical application such as cross sensitivity towards other metal ions, longer response times, low water solubility, a narrow pH span, tricky procedures for synthesis and poor sensitivity [19–21]. In addition, some “turn-off” fluorescent probes can only be applied in non-aqueous solvents which limit their application in biological systems [22, 23]. Thus it is of significance to develop fluorescent probes that would allow accurate, sensitive, rapid recognition of Cu<sup>2+</sup> in aqueous media.

The pyrazoline-based fluorescent probes have attracted considerable interest because of their blue light emission with high fluorescence quantum yield [24–27]. Consequently, several pyrazoline-based probes for metal ions, such as Zn<sup>2+</sup> [28] have been studied. However, some of them were used with no success in biological applications. As an extension of our work on the development of fluorescent probe for monitoring metal ions [29–33], herein we report the design and synthesis of a new pyrazoline-based fluorescent probes **4** (Scheme 1) for Cu<sup>2+</sup> recognition. Probe **4** is not only of

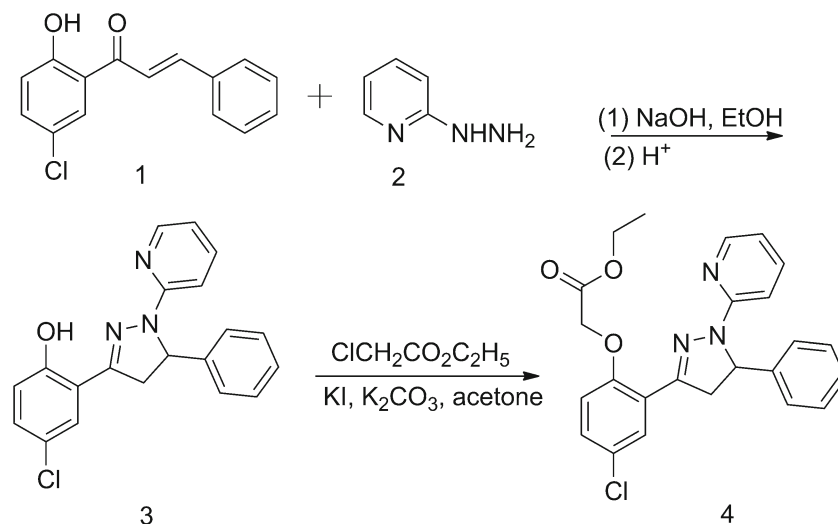
---

Meng-Meng Li and Shu-Ya Huang contributed equally.

**Electronic supplementary material** The online version of this article (doi:10.1007/s10895-013-1203-0) contains supplementary material, which is available to authorized users.

M.-M. Li · H. Ye · F. Ge · B.-X. Zhao (✉)  
Institute of Organic Chemistry, School of Chemistry and Chemical Engineering, Shandong University, Jinan 250100, People’s Republic of China  
e-mail: bxzhao@sdu.edu.cn

S.-Y. Huang · J.-Y. Miao (✉)  
Institute of Developmental Biology, School of Life Science, Shandong University, Jinan 250100, People’s Republic of China  
e-mail: miaojy@sdu.edu.cn

**Scheme 1** Synthesis of compound **4**

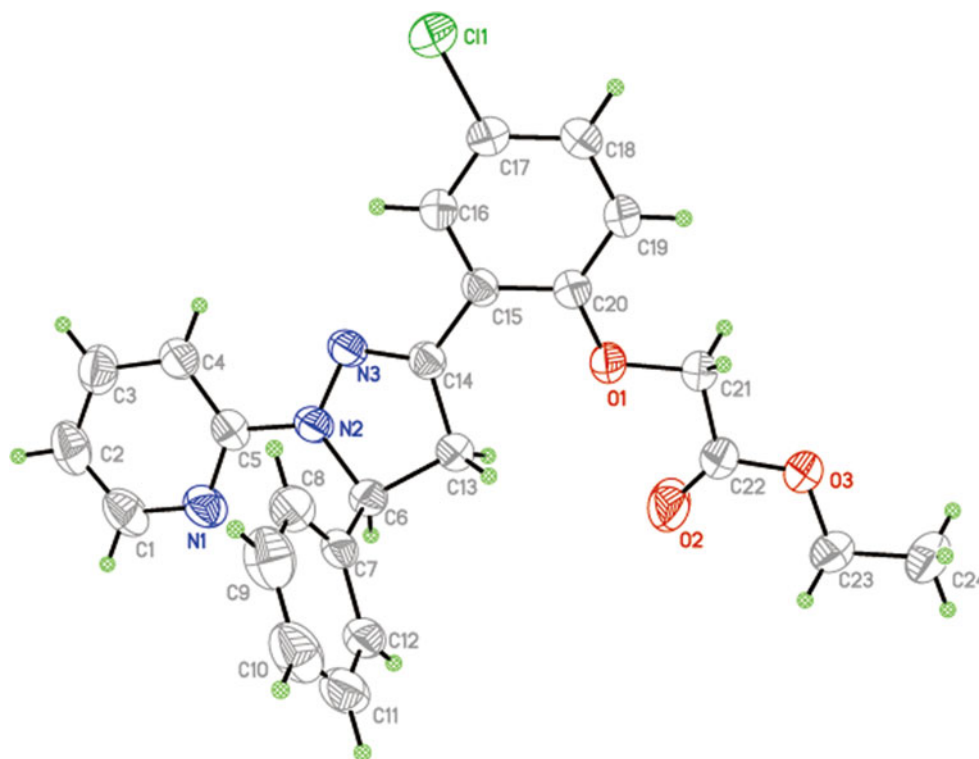
high sensitivity and selectivity in aqueous media but also can detect Cu<sup>2+</sup> in living cells.

## Experimental Details

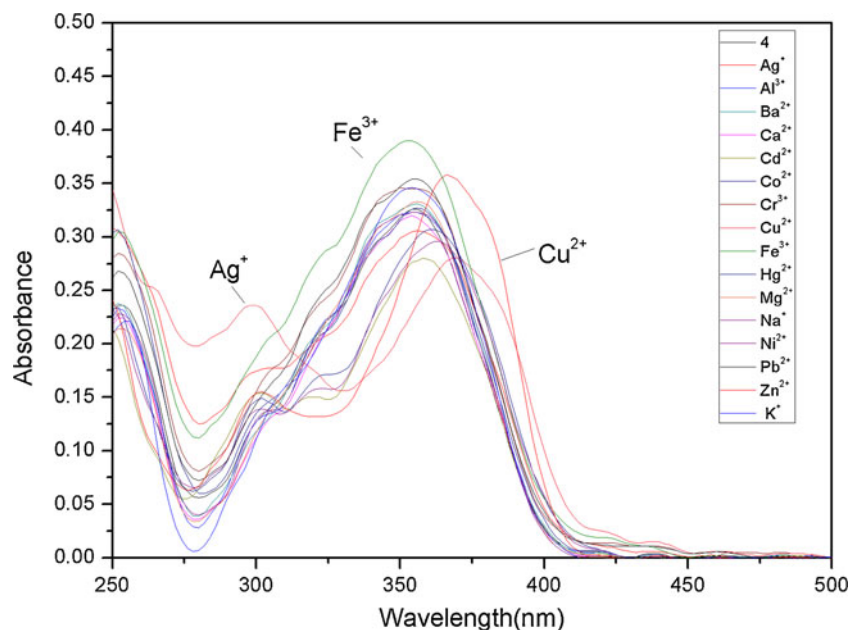
### Apparatus

Thin-layer chromatography (TLC) was conducted on silica gel 60 F<sub>254</sub> plates (Merck KGaA). <sup>1</sup>H NMR spectra were recorded on a Bruker Avance 400 (400 MHz) spectrometer, using DMSO as solvent. <sup>13</sup>C NMR spectra were recorded on

a Bruker Avance 300 (75 MHz) spectrometer, using CDCl<sub>3</sub> as solvent, and tetramethylsilane (TMS) as internal standard. Melting points were determined on an XD-4 digital micro melting point apparatus. IR spectra were recorded with an IR spectrophotometer VERTEX 70 FT-IR (Bruker Optics). HRMS spectra were recorded on a QTOF6510 spectrograph (Agilent). UV–vis spectra were recorded on a U-4100 (Hitachi). Fluorescent measurements were recorded on a Perkin–Elmer LS-55 luminescence spectrophotometer. All pH measurements were made with a Model PHS-3C pH meter (Shanghai, China) and operated at room temperature about 298 K.

**Fig. 1** Crystal structure of **4**

**Fig. 2** Absorption spectra of **4** (20  $\mu$ M) in buffered EtOH/HEPES solution (20 mM, pH=7.2, 2:3, v/v) with 5 equiv. of metal ions:  $\text{Al}^{3+}$ ,  $\text{Fe}^{3+}$ ,  $\text{Co}^{2+}$ ,  $\text{Ni}^{2+}$ ,  $\text{Ba}^{2+}$ ,  $\text{Ca}^{2+}$ ,  $\text{Cd}^{2+}$ ,  $\text{Cr}^{3+}$ ,  $\text{K}^+$ ,  $\text{Mg}^{2+}$ ,  $\text{Na}^+$ ,  $\text{Ag}^+$ ,  $\text{Hg}^{2+}$ ,  $\text{Zn}^{2+}$ ,  $\text{Cu}^{2+}$  ions and blank



### Reagents

Deionized water was used throughout the experiment. All the reagents were purchased from commercial suppliers and used without further purification. The salts used in stock aqueous solutions of metal ions were  $\text{NaNO}_3$ ,  $\text{Fe}(\text{NO}_3)_3 \cdot 9\text{H}_2\text{O}$ ,  $\text{AgNO}_3$ ,  $\text{KNO}_3$ ,  $\text{Co}(\text{NO}_3)_2 \cdot 6\text{H}_2\text{O}$ ,  $\text{Mg}(\text{NO}_3)_2 \cdot 6\text{H}_2\text{O}$ ,  $\text{Ca}(\text{NO}_3)_2 \cdot 4\text{H}_2\text{O}$ ,  $\text{Al}(\text{NO}_3)_3 \cdot 9\text{H}_2\text{O}$ ,  $\text{Ba}(\text{NO}_3)_2$ ,  $\text{Cr}(\text{NO}_3)_3 \cdot 9\text{H}_2\text{O}$ ,  $\text{Ni}(\text{NO}_3)_2 \cdot 6\text{H}_2\text{O}$ ,  $\text{Cd}(\text{NO}_3)_2 \cdot 4\text{H}_2\text{O}$ ,  $\text{Pb}(\text{NO}_3)_2$ ,  $\text{Cu}(\text{NO}_3)_2 \cdot 3\text{H}_2\text{O}$ ,  $\text{Zn}(\text{NO}_3)_2 \cdot 6\text{H}_2\text{O}$  and  $\text{HgCl}_2$ .

Synthesis of Ethyl 2-(4-chloro-2-(5-phenyl-1-(pyridin-2-yl)-4,5-dihydro-1H-pyrazol-3-yl)phenoxy)Acetate (**4**)

The synthetic route of the proposed compound **4** is shown in Scheme 1. Starting material pyrazoline (**3**) was prepared according to the literature [31]. A mixture pyrazoline (**3**) (0.350 g, 1 mmol), KI (0.168 g, 1 mmol),  $\text{K}_2\text{CO}_3$  (0.331 g, 2.4 mmol), ethyl chloroacetate (0.150 g, 1.2 mmol) and acetone (25 ml) was stirred at reflux for 2 h. After cooling, the mixture was filtered and the filtrate was evaporated to afford

**Fig. 3** Fluorescence emission spectra of **4** (10  $\mu$ M) in buffered EtOH/HEPES (20 mM, pH=7.2, 2:3, v/v) solution with 5 equiv. of metal ions:  $\text{Al}^{3+}$ ,  $\text{Fe}^{3+}$ ,  $\text{Co}^{2+}$ ,  $\text{Ni}^{2+}$ ,  $\text{Ba}^{2+}$ ,  $\text{Ca}^{2+}$ ,  $\text{Cd}^{2+}$ ,  $\text{Cr}^{3+}$ ,  $\text{K}^+$ ,  $\text{Mg}^{2+}$ ,  $\text{Na}^+$ ,  $\text{Ag}^+$ ,  $\text{Hg}^{2+}$ ,  $\text{Zn}^{2+}$ ,  $\text{Cu}^{2+}$  ions and blank. Excitation wavelength was 354 nm. Emission wavelength was 445 nm. Inset: the color change of color **4** (10  $\mu$ M) in buffered EtOH/HEPES (20 mM, pH=7.2, 2:3, v/v) solution with 5 equiv.  $\text{Cu}^{2+}$

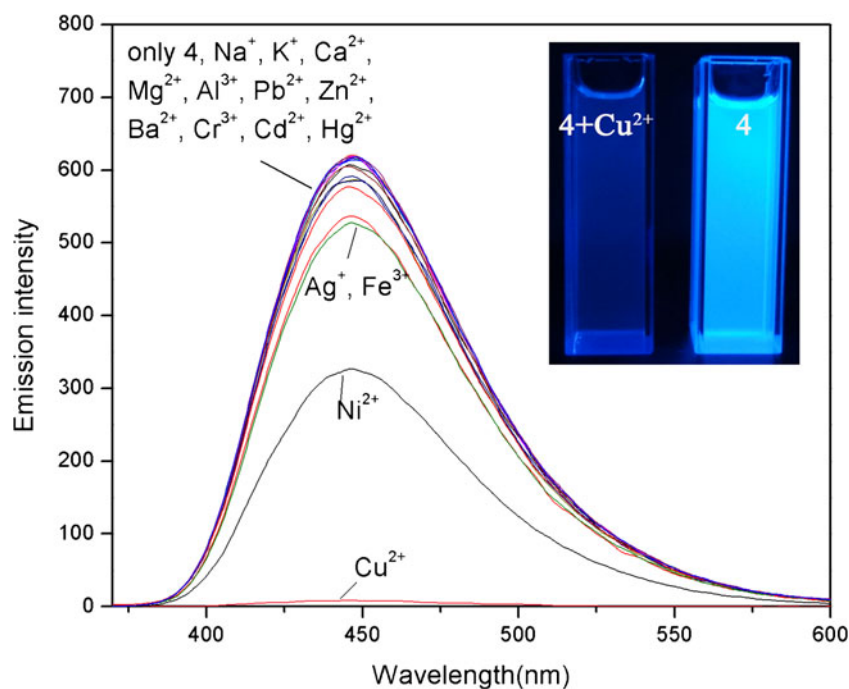
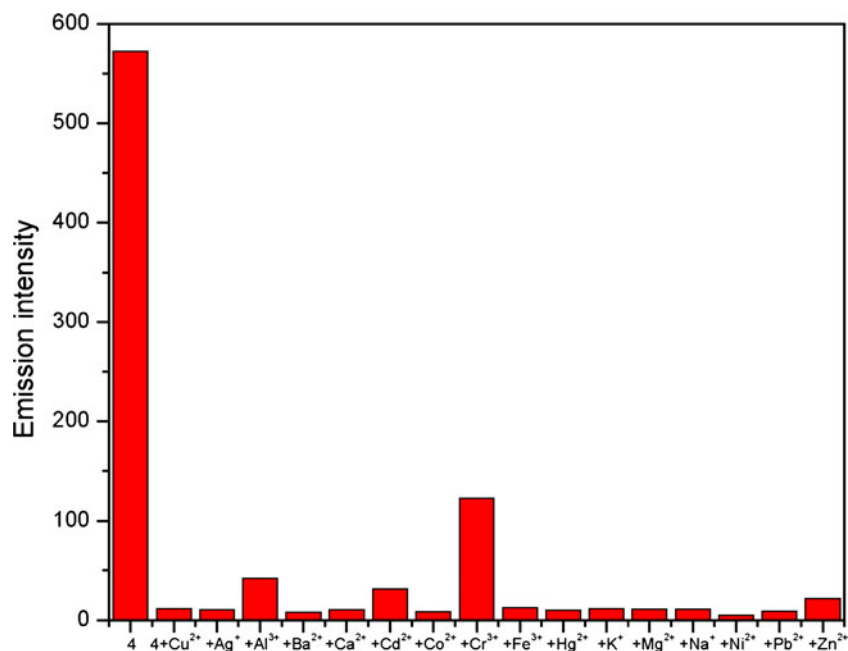


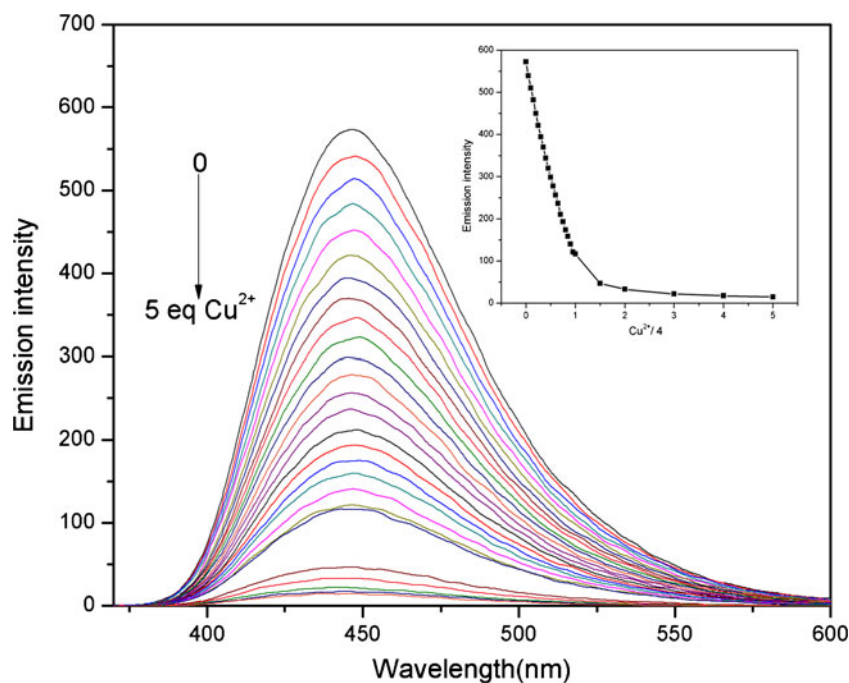
**Fig. 4** Fluorescence emission spectra of **4** (10  $\mu\text{M}$ ) in buffered EtOH/HEPES (20 mM, pH=7.2, 2:3, v/v) solution containing 5 equiv. of  $\text{Cu}^{2+}$  to the selected metal ions  $\text{Al}^{3+}$ ,  $\text{Fe}^{3+}$ ,  $\text{Co}^{2+}$ ,  $\text{Ni}^{2+}$ ,  $\text{Ag}^+$ ,  $\text{Hg}^{2+}$ ,  $\text{Zn}^{2+}$ ,  $\text{Ba}^{2+}$ ,  $\text{Cd}^{2+}$ ,  $\text{Cr}^{3+}$  (5 equiv.) and  $\text{Mg}^{2+}$ ,  $\text{Ca}^{2+}$ ,  $\text{K}^+$ ,  $\text{Na}^+$  (50 equiv.). Excitation wavelength was 354 nm. Emission wavelength was 445 nm



residue. The residue was crystallized from ethanol to afford **4** (0.227 g), Yield: 55.2 %; mp: 158–160  $^{\circ}\text{C}$ ; IR (KBr,  $\text{cm}^{-1}$ ): 3501.7, 2924.2, 1764.5, 1590.2, 1481.8, 1417.8, 1219.8, 1137.4, 1075.3, 765.4, 700.3;  $^1\text{H}$  NMR (400 MHz, DMSO):  $\delta$  1.14 (t, 3H,  $J=7.04$  Hz,  $\text{CH}_3$ ), 3.34 (dd, 1H,  $J=5.28$ , 18.60 Hz, 4-*Htrans*), 4.03 (dd, 1H,  $J=12.28$ , 18.60 Hz, 4-*Hcis*), 4.12 (q, 2H,  $J=7.11$  Hz,  $\text{CO}_2\text{CH}_2$ ), 4.84 (s, 2H,  $\text{OCH}_2\text{CO}$ ), 5.72 (dd, 1H,  $J=5.28$ , 12.28 Hz, 5-H of pyrazoline), 6.69 (t, 1H,  $J=6$  Hz, pyridine-H), 7.09 (d, 1H,

$J=8.88$  Hz, Ar-H), 7.17–7.22 (m, 3H, Ar-H), 7.2–7.30 (m, 2H, Ar-H), 7.39 (dd, 1H,  $J=2.8$ , 6 Hz, Ar-H), 7.46 (d, 1H,  $J=8.56$  Hz, Ar-H), 7.60 (t, 1H,  $J=4.34$  Hz, Ar-H), 7.95 (d, 1H,  $J=2.84$  Hz, Ar-H), 7.97 (s, 1H, Ar-H),  $^{13}\text{C}$  NMR (75 MHz,  $\text{CDCl}_3$ ): 167.96, 155.17, 154.26, 147.86, 147.39, 143.19, 137.23, 129.60, 128.65, 128.61 (2C), 127.16, 127.00, 125.81 (2C), 123.99, 114.48, 113.70, 109.27, 77.43, 77.01, 76.58, 65.90, 62.25, 61.52, 45.54, 14.08; HRMS: calcd for  $[\text{M}+\text{H}]^+$   $\text{C}_{24}\text{H}_{23}\text{ClN}_3\text{O}_3$ : 436.1428; found: 436.1409.

**Fig. 5** Fluorescence emission spectra of **4** (10  $\mu\text{M}$ ) upon the addition of  $\text{Cu}^{2+}$  (0–5 equiv.) in buffered EtOH/HEPES (20 mM, pH=7.2, 2:3, v/v) solution. The inset shows the emission of **4** at 445 nm as a function of  $\text{Cu}^{2+}$  concentration



A single crystal of **4** was obtained from an ethanol solution and was characterized using X-ray crystallography (Fig. 1).

### Cell Culture and Imaging

Hela cells were cultured in Dulbecco's modified Eagle's medium (DMEM, Gibco) containing 10 % calf bovine serum (HyClone) at 37 °C in humidified air and 5 % CO<sub>2</sub>. For fluorescence imaging, the cells ( $5 \times 10^4 \text{ mL}^{-1}$ ) were seeded into 24-well plates, and experiments to assay Cu<sup>2+</sup> uptake were performed in the same media supplemented with 1 μM of CuCl<sub>2</sub> for 0.5 h. The cells were washed twice with PBS buffer before the staining experiments, and incubated with 1 μM of probe **4** for 1 h in the incubator. After washing twice with PBS, the cells were imaged under a Phase Contrast Microscope (Nikon, Japan).

## Results and Discussion

### Absorption Properties

As shown in Fig. 2, free probe **4** exhibits a maximum absorption wavelength at 354 nm in buffered EtOH/HEPES solution (20 mM, pH=7.2, 2:3, v/v). Upon addition of Cu<sup>2+</sup> or Ag<sup>+</sup>, a maximum absorption at 370 nm appeared. The addition of other metal ions such as Al<sup>3+</sup>, Fe<sup>3+</sup>, Co<sup>2+</sup>, Ni<sup>2+</sup>, Ba<sup>2+</sup>, Ca<sup>2+</sup>, Cd<sup>2+</sup>, Cr<sup>3+</sup>, K<sup>+</sup>, Mg<sup>2+</sup>, Na<sup>+</sup>, Hg<sup>2+</sup>, Zn<sup>2+</sup> had little change to the UV–vis spectrum of **4**. In addition, during the UV–vis spectrum of **4** with different concentration, the absorption maximum shows at 354 nm and the  $\epsilon$  is  $2.7 \times 10^4 \text{ M}^{-1} \text{ cm}^{-1}$  (Fig. S1, Fig. S2).

### Selectivity Studies

The fluorescence spectrum changes of probe **4** (10 μM) in buffered EtOH/HEPES solution (20 mM, pH=7.2, 2:3, v/v) before and after addition of different metal ions were examined. As shown in Fig. 3, free probe **4** shows a strong fluorescence emission at 445 nm. Interestingly, addition of 5 equiv. of Cu<sup>2+</sup> resulted in a remarkably quenching of fluorescence intensity. However, the addition of other metal ions such as Al<sup>3+</sup>, Fe<sup>3+</sup>, Co<sup>2+</sup>, Ba<sup>2+</sup>, Ca<sup>2+</sup>, Cd<sup>2+</sup>, Cr<sup>3+</sup>, K<sup>+</sup>,

**Scheme 2** The proposed binding mode

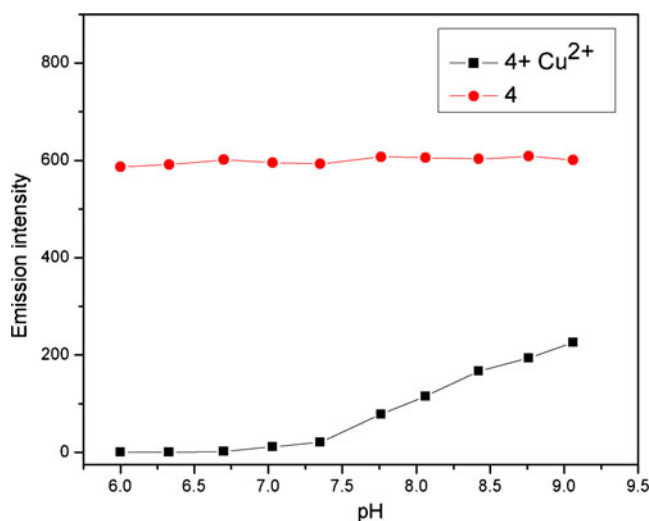
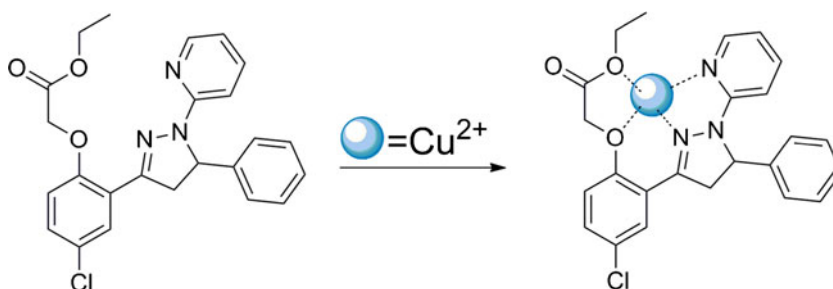


**Fig. 6** The effect of pH (6.0–9.06) on the relative fluorescence intensity probe **4** with 5 equiv. Cu<sup>2+</sup> in buffered EtOH/HEPES (20 mM, pH=7.2, 2:3, v/v) solution. Excitation wavelength was 354 nm. Emission wavelength was 445 nm

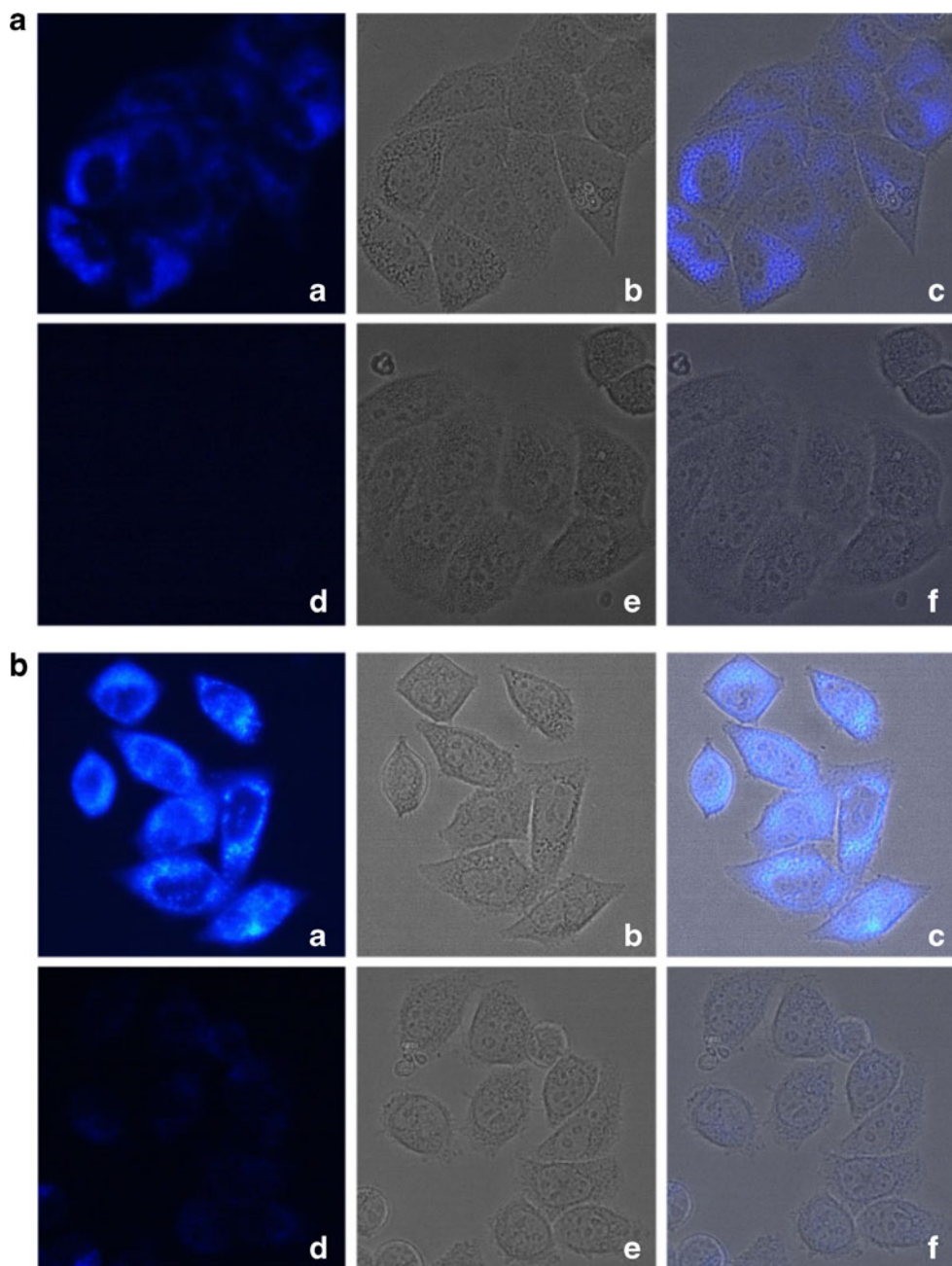
Mg<sup>2+</sup>, Na<sup>+</sup>, Ag<sup>+</sup>, Hg<sup>2+</sup>, Zn<sup>2+</sup> with the same concentration does not trigger obvious fluorescence change of the probe, which well illustrates the selectivity of the probe to Cu<sup>2+</sup>. The phenomenon was also justified by the change in color from stronger blue emission to almost dark in presence of Cu<sup>2+</sup> under the irradiation at 365 nm (Fig. 3 inset).

Interestingly, upon addition of different anions (1 equiv.) such as CuSO<sub>4</sub>, CuCl<sub>2</sub>, Cu(NO<sub>3</sub>)<sub>2</sub> and Cu(OAc)<sub>2</sub> to a solution of probe **4** (10 μM), no significant change in the optical properties was observed (Fig. S3). So the copper salts with different anions all can quench the fluorescence intensity of probe **4**.

### Tolerance Over Other Metal Ions

To check the practical ability of probe **4** as a Cu<sup>2+</sup> selective fluorescent chemosensor, the competition experiments were carried out in the presence of 5 equiv. Cu<sup>2+</sup> mixed with other competing metal ions. As shown in Fig. 4, only Cr<sup>3+</sup> slightly disturbed the intensity of **4**-Cu (II) and the initial fluorescence intensity of **4**-Cu (II) did not changed significantly with other metal ions such as Al<sup>3+</sup>, Fe<sup>3+</sup>, Co<sup>2+</sup>, Ni<sup>2+</sup>, Ba<sup>2+</sup>, Ca<sup>2+</sup>, Cd<sup>2+</sup>, K<sup>+</sup>, Mg<sup>2+</sup>, Na<sup>+</sup>, Ag<sup>+</sup>, Hg<sup>2+</sup>, Zn<sup>2+</sup>. This indicated

**Fig. 7** Fluorescence microscope images of living HeLa cells. **a** using 1  $\mu\text{M}$  probe and 2  $\mu\text{M}$   $\text{Cu}(\text{NO}_3)_2$ ; **b** using 5  $\mu\text{M}$  probe and 10  $\mu\text{M}$   $\text{Cu}(\text{NO}_3)_2$ . **a** Cells incubated with probe **4** for 2 h at 37°C; **b** Bright-field view of panel (a); **c** Overlay image of (a) and (b). **d** Cells incubated with probe for 2 h at 37°C and then incubated with  $\text{Cu}^{2+}$  added to the growth medium for 30 min at 37°C. **e** Bright-field image of the live HeLa cells shown in panel (d). **f** Overlay image of (d) and (e)



that probe **4** had a high selectivity for  $\text{Cu}^{2+}$  in the presence of other related species.

#### $\text{Cu}^{2+}$ -titration

To further investigate the interaction of probe **4** and  $\text{Cu}^{2+}$ , a fluorescence titration experiment was carried out, as shown in Fig. 5. With increasing the  $\text{Cu}^{2+}$  concentration, the original strong fluorescence emission at 445 nm was gradually quenched and it was quenched almost completely after the addition of 1 equiv.  $\text{Cu}^{2+}$ . And when the  $\text{Cu}^{2+}$  concentration increased up to 5

equiv., the fluorescence emission did not cause significant changes.

#### The Proposed Reaction Mechanism

To investigate the probable complexation of the probe **4** with  $\text{Cu}^{2+}$ , the binding model of the probe **4** and  $\text{Cu}^{2+}$  was proposed as shown in Scheme 2. The probe is the most likely to chelate  $\text{Cu}^{2+}$  via its oxygen on the ether, oxygen on the carbonyl group, as well as nitrogen on the pyridine and pyrazoline. This binding mode was further supported by a Job's plot. As shown in Fig. S4, the

absorbance reached a inflection point when the ratio was 0.5, which indicated a 1:1 stoichiometry of the  $\text{Cu}^{2+}$  to 4 in the complex [16].

#### Kinetic Assay and Effect of pH

The spectra response of probe 4 in the absence and presence of  $\text{Cu}^{2+}$  in different pH values were firstly evaluated. As shown in Fig. 6, in the pH range of 6.0–9.06, obvious characteristic emission of 4 could be observed. However, the addition of  $\text{Cu}^{2+}$  led to the fluorescence quenching over a comparatively wide pH range (6.0–7.5). It means that probe 4 can serve as a good selective chemosensor for  $\text{Cu}^{2+}$  in near neutral and weak acidic medium, which is important in both environmental and biological analysis. Further, the time-dependence of fluorescence of probe 4 was also evaluated in the presence of  $\text{Cu}^{2+}$ . As shown in Fig. S5,  $\text{Cu}^{2+}$  induced fluorescence quenching can complete within 10 min after addition of  $\text{Cu}^{2+}$ . This suggests that probe 4 could be used for real-time tracking of  $\text{Cu}^{2+}$  in cells.

#### Linear Range and Limit Of Detection

Generally, as a highly selective and sensitive fluorescent probe, the detection limit is an important factor in practical application. As shown in Fig. S6, the limit of detection of probe 4 for  $\text{Cu}^{2+}$  is measured to be  $3.74 \times 10^{-7} \text{M}$ , and the correlation coefficient is 0.997 [34].

The binding stoichiometry of probe 4 with  $\text{Cu}^{2+}$  was calculated through the Benesi–Hildebrand equation [35]. As shown in Fig. S7, when the  $\text{Cu}^{2+}$  concentration ranged from 4  $\mu\text{M}$  to 8.5  $\mu\text{M}$ , the plot of  $1/(I_0 - I)$  against  $1/[\text{Cu}^{2+}]$  shows a linear relationship, which demonstrates that probe 4 coordinated with  $\text{Cu}^{2+}$  in a 1:1 ratio, and the binding constant was calculated from the ratio of intercept/slope to be  $1.49 \times 10^4 \text{M}^{-1}$  with the correlation coefficient as high as 0.9991. Thus the fact suggests the high copper affinity of probe 4 as speculated.

#### Imaging of Intracellular $\text{Cu}^{2+}$

The ability of probes to sensitively and selectively detect analyte in living cells is significant for biological application. Considering that higher level of  $\text{Cu}^{2+}$  in tumors takes a possible key role in promoting angiogenesis, we carried out experiment using the probe on HeLa cells.

From Fig. 7, we can clearly observe significant confocal imaging changes of probe 4 (1 and 5  $\mu\text{M}$ ) in the medium upon addition of  $\text{Cu}^{2+}$  (2 equiv.) for 2 h at 37 °C. HeLa cells incubated with probe 4 initially display a strong fluorescent image, but the fluorescence image completely quenched in the presence of  $\text{Cu}^{2+}$ . Moreover, with increasing concentration of the probe 4 incubated, fluorescence intensity enhanced

obviously in concentration-dependent manner and at the presence of  $\text{Cu}^{2+}$  fluorescence images of the cells revealed a remarkable quenching. These results demonstrate that probe 4 can be useful for monitoring  $\text{Cu}^{2+}$  in living cells.

#### Conclusion

In summary, we have developed a highly sensitive and selective probe for  $\text{Cu}^{2+}$  in aqueous solution. The change in color of solution from fluorescent blue to a non-fluorescent was readily distinguishable. Job's plot confirmed the presence of  $\text{Cu}^{2+}$  induced the formation of complex in the 1:1 binding mode. When 10  $\mu\text{M}$  of probe 4 was used in buffered EtOH/HEPES (20 mM, pH=7.2, 2:3, v/v) solution, the detection limit was low to 0.4  $\mu\text{M}$ . Meanwhile, the experimental results demonstrate that probe 4 could be used to detect  $\text{Cu}^{2+}$  in living cells.

**Acknowledgments** This study was supported by 973 Program (2010CB933504) and National Natural Science Foundation of China (90813022 and 20972088).

#### References

1. Kumar S, Singh P, Kaur S (2007) A  $\text{Cu}^{2+}$  protein cavity mimicking fluorescent chemosensor for selective  $\text{Cu}^{2+}$  recognition: tuning of fluorescence quenching to enhancement through spatial placement of anthracene unit. *Tetrahedron* 63:11724–11732
2. Kaur N, Kumar S (2006) Colorimetric recognition of Cu(II) by (2-dimethylaminoethyl)amino appended anthracene-9,10-diones in aqueous solutions: deprotonation of aryl amine NH responsible for colour changes. *Dalton Trans* 31:3766–3771
3. Qi JJ, Han MS, Tung CH (2012) A benzothiazole alkyne fluorescent sensor for Cu detection in living cell. *Bioorg Med Chem Lett* 22:1747–1749
4. Gaggelli E, Kozłowski H, Valensin D, Valensin G (2006) Copper homeostasis and neurodegenerative disorders (Alzheimer's, prion, and Parkinson's diseases and amyotrophic lateral sclerosis). *Chem Rev* 106:1995–2044
5. Desai V, Kaler SG (2008) Role of copper in human neurological disorders. *Am J Clin Nutr* 88:855–858
6. Bruijn LI, Miller TM, Cleveland DW (2004) Unraveling the mechanisms involved in motor neuron degeneration in ALS. *Ann Rev Neurosci* 27:723–749
7. Ahamed BN, Ghosh P (2011) Selective colorimetric and fluorometric sensing of Cu (II) by iminocoumarin derivative in aqueous buffer. *Dalton Trans* 40:641–6419
8. De Silva AP, Gunaratne HQN, Gunnlaugsson T, Huxley AJM, McCoy CP, Rademacher JT (1997) Signaling recognition events with fluorescent sensors and switches. *Chem Rev* 97:1515–1516
9. Basabe-Desmonts L, Reinhoubt DN, Crego-Calama M (2007) Design of fluorescent materials for chemical sensing. *Chem Soc Rev* 36:993–1017
10. Yu FB, Zhang WS, Li P, Xing YL, Tong LL, Ma JP, Tang B (2009)  $\text{Cu}^{2+}$ -selective naked-eye and fluorescent probe: its crystal structure and application in bioimaging. *Analyst* 134:1826–1833

11. Mahapatra AK, Roy J, Manna SK, Kundu S, Sahoo P, Mukhopadhyay SK, Banik A (2012) Hg<sup>2+</sup>-selective “turn-on” fluorescent chemodosimeter derived from glycine and living cell imaging. *Photochem Photobiol A Chem* 240:26–32
12. Paul BK, Kar S, Guchhait N (2011) A Schiff base-derived new model compound for selective fluorescence sensing of Cu(II) and Zn(II) with ratiometric sensing potential: synthesis, photophysics and mechanism of sensory action. *Photochem Photobiol A Chem* 220:153–163
13. Fan JL, Liu XJ, Hu MM, Zhu H, Song FL, Peng XJ (2012) Development of an oxidative dehydrogenation-based fluorescent probe for Cu<sup>2+</sup> and its biological imaging in living cells. *Anal Chim Acta* 735:107–113
14. Yu CW, Wang T, Xu K, Zhao J, Li MH, Weng SX, Zhang J (2013) Characterization of a highly Cu<sup>2+</sup>-selective fluorescent probe derived from rhodamine B. *Dyes Pigments* 96:38–44
15. Yuan L, Lin WY, Chen B, Xie YN (2012) Development of FRET-based ratiometric fluorescent Cu<sup>2+</sup> chemodosimeters and the applications for living cell imaging. *Org Lett* 14:432–435
16. Li P, Zhou H, Tang B (2012) A lysosomal-targeted fluorescent probe for detecting Cu<sup>2+</sup>. *Photochem Photobiol A Chem* 249:36–40
17. Jung HS, Kwon PS, Lee JW, Kim J, Hong CS, Kim JW, Yan SH, Lee JY, Lee JH, Joo TH, Kim JS (2009) Coumarin-derived Cu<sup>2+</sup>-selective fluorescence sensor: synthesis, mechanisms, and applications in living cells. *J Am Chem Soc* 131:2008–2012
18. Varnes AW, Dodson RB, Wehry EL (1972) Interactions of transition-metal ions with photoexcited states of flavines. Fluorescence quenching studies. *J Am Chem Soc* 94:946–950
19. Wang HX, Yang L, Zhang WB, Zhou Y, Zhao B, Li XY (2012) A colorimetric probe for copper(II) ion based on 4-amino-1,8-naphthalimide. *Inorg Chim Acta* 381:111–116
20. Kim SH, Kim JS, Park SM, Chang SK (2006) Hg<sup>2+</sup>-selective off-on and Cu<sup>2+</sup>-selective on-off type fluoroionophore based upon cyclam. *Org Lett* 8:371–374
21. Luo Y, Li Y, Lv BQ, Zhou ZD, Xiao D, Choi MMF (2009) A new luminol derivative as a fluorescent probe for trace analysis of copper (II). *Microchim Acta* 164:411–417
22. Shao N, Pang GX, Wang XR, Wu RJ, Cheng Y (2010) Dimerization of 2-pyridylisonitriles produces p-extended fused heteroarenes useful as highly selective colorimetric and optical probes for copper ion. *Tetrahedron* 66:7302–7308
23. Mu HL, Gong R, Ma Q, Sun YM, Fu EQ (2007) A novel colorimetric and fluorescent chemosensor: synthesis and selective detection for Cu<sup>2+</sup> and Hg<sup>2+</sup>. *Tetrahedron Lett* 48:5525–5529
24. Ji SJ, Shi HB (2006) Synthesis and fluorescent property of some novel benzothiazoyl pyrazoline derivatives containing aromatic heterocycle. *Dyes Pigments* 70:246–250
25. Bian B, Ji SJ, Shi HB (2008) Synthesis and fluorescent property of some novel Bischromophore compounds containing pyrazoline and naphthalimide groups. *Dyes Pigments* 76:348–352
26. Svehkarev DA, Ilya V, Bukatich AO (2008) Doroshenko, new 1,3,5-triphenyl-2-pyrazoline-containing 3-hydroxychromones as highly solvatofluorochromic ratiometric polarity probes. *J Photochem Photobiol A Chem* 200:426–431
27. Song SM, Ju D, Li JF, Li DX, Wei YL, Dong C, Lin PH, Shuang SM (2009) Synthesis and spectral characteristics of two novel intramolecular charge transfer fluorescent dyes. *Talanta* 77:1707–1714
28. Gong ZL, Zhao BX, Liu WY, Lv HS (2011) A new highly selective “turn on” fluorescent sensor for zinc ion based on a pyrazoline derivative. *J Photochem Photobiol A Chem* 218:6–10
29. Liu WY, Li HY, Zhao BX, Miao JY (2012) A new fluorescent and colorimetric probe for Cu<sup>2+</sup> in live cells. *Analyst* 137:3466–3469
30. Liu WY, Li HY, Lv HS, Zhao BX, Miao JY (2012) A rhodamine chromene-based turn-on fluorescence probe for selectively imaging Cu<sup>2+</sup> in living cell. *Spectrochim Acta A* 95:658–663
31. Gong ZL, Ge F, Zhao BX (2011) Novel pyrazoline-based selective fluorescent sensor for Zn<sup>2+</sup> in aqueous media. *Sensor Actuat B* 159:48–153
32. Liu WY, Li HY, Zhao BX, Miao JY (2011) Synthesis, crystal structure and living cell imaging of a Cu<sup>2+</sup>-specific molecular probe. *Org Biomol Chem* 9:4802–4805
33. Zhang Z, Wang FW, Wang SQ, Ge F, Zhao BX, Miao JY (2012) A highly sensitive fluorescent probe based on simple pyrazoline for Zn<sup>2+</sup> in living neuron cells. *Org Biomol Chem* 10:8640–8644
34. Zhang D, Wang M, Chai MM, Chen XP, Ye Y, Zhao YF (2012) Three highly sensitive and selective colorimetric and off-on fluorescent chemosensors for Cu<sup>2+</sup> in aqueous solution. *Sensor Actuat B* 168:200–206
35. Benesi HA, Hildebrand JH (1949) A spectrophotometric investigation of the interaction of iodine with aromatic hydrocarbons. *J Am Chem Soc* 71:2703–2707